Journal of Applied Mathematics and Mechanics 74 (2010) 223–231

Contents lists available at ScienceDirect

Journal of Applied Mathematics and Mechanics

journal homepage: www.elsevier.com/locate/jappmathmech

The end zone of a shear crack propagating at an intersonic velocity☆

A.M. Lin'kov

St. Petersburg, Russia

ARTICLE INFO

Article history:
Received 13 August 2008

ABSTRACT

An asymptotic solution of the problem for a shear crack propagating at an intersonic velocity is given that determines the size of the end zone, the distribution of the displacement jump in it and the dependence of the propagation velocity on an effective stress intensity factor, introduced in this paper. Numerical data are presented for the case of linear softening in the end zone and a comparison is made with the results for the Leonov–Panasyuk–Dugdale model. It is established using an effective stress intensity factor that the propagation is unstable at velocities close to the velocity of transverse waves; it becomes stable when approaching the velocity of longitudinal waves.

It has been shown[1–3] that steady propagation is impossible over the range of velocities from the Rayleigh velocity to the velocity of transverse waves in the case of a shear crack in a homogeneous isotropic medium. The transition into the intersonic region can therefore only be accomplished by a jump. The question as to whether such a jump occurs in practice remains open. The lack of any general theoretical foundations prohibiting a transition into the intersonic zone suggests a positive answer to this question. Such a transition has been numerically modelled in the case of a homogeneous medium.[4,5] For media with *dissimilar* properties, the crack propagation at an intersonic velocity along the contact of the media has been observed in experiments.[6–8] This all stimulates a theoretical investigation of the special features of the motion of a shear crack in the intersonic zone.

The first theoretical investigation of the end zone of a shear crack at arbitrary velocities[1] led to the derivation of asymptotic equations, the construction of their solutions for models of linear and non-linear softening in the end zone and to the acquisition of numerical data on the distribution of the displacement discontinuities and the relation between the concentrated external force and the velocity of the crack. However, the authors started out from a singular solution which gave a finite stress at the crack tip and an infinite jump in the displacements at infinity. This eliminated the possibility of using the stress intensity factor (SIF) and did not allow the link with classical crack theory to be established either in the subsonic or intersonic domains. An alternative singular solution, in which the displacement jump remains finite at infinity while the stresses at the tip become infinite, has been investigated for the subsonic region[9,10] and for a whole range of velocities.[3] Some numerical data on an end zone with linear softening have been presented,[3] but the graphs shown were primarily aimed at establishing the error in the proposed approximate approach,[3] which involved the use of a dispersion relation for the softening contact. No detailed analysis of the special features of crack propagation in the intersonic region and its relation to the SIF has been carried out.

A general asymptotic solution of the problem of crack propagation along the boundary of media with arbitrary properties was presented in Ref. 2. The problem of a crack in a homogeneous medium was considered as one of the illustrations. The Leonov–Panasyuk–Dugdale model (called the Dugdale model in Ref. 2) was used with the aim of obtaining simple analytical relations. Unfortunately, an error was made in the analytical solution of the Riemann–Hilbert problem for this model, since an important terms outside the integral, which corresponds to a delta-function and which is present in the solutions in Refs 1–3, was not included. Although this term vanishes at a velocity less than the velocity of transverse waves and is close to zero over a large part of the intersonic range, it is important in cases when the velocity is close to the velocity of transverse or longitudinal waves.

In this paper, these gaps in the investigation of the intersonic region are filled in. To be precise, firstly, detailed numerical data and an analysis of the special features of the end zone are presented for the case of linear softening in this zone and, secondly, a comparison with the results for the Leonov–Panasyuk–Dugdale model is made. In passing, the concept of an effective stress intensity factor is introduced which follows from the form of the asymptotic relations and the condition for the stresses at the crack tip to be finite.

☆ Prikl. Mat. Mekh. Vol. 74, No. 2, pp. 311-323, 2010.
E-mail address: linkova@hotmail.com.

0021-8928/$ – see front matter © 2010 Elsevier Ltd. All rights reserved.
doi:10.1016/j.jappmathmech.2010.05.013

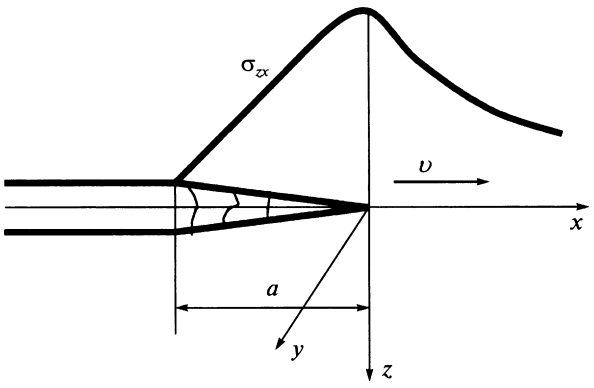

Fig. 1.

1. Asymptotic relations for the end zone of a moving shear crack

Consider a shear crack, the tip of which, at the instant under consideration, has a velocity υ and has advanced sufficiently far that the field in the neighbourhood of the front can be considered as being a locally steady field (Fig. 1). We will use a right-handed system of coordinates x, y, z which moves together with the crack tip, with the x axis along the direction of motion of the fracture, the y axis along the front and the z axis perpendicular to the fracture plane. The following notation is used: $\Delta u_x = u_x^+ - u_x^-$ is the jump in the tangential displacements, and σ_{zx} are the shear forces, which remain continuous on passing across the surface of the crack (they can be discontinuous along a crack and correspond to a concentrated force). There is no displacement jump ahead of the front: $\Delta u_x = 0$ when $x \geq 0$. Suppose the forces are equal to zero behind the front with the exception of the point x_0 where an isolated concentrated force is applied which follows the crack tip $\sigma_{zx} = \delta(x - x_0)$, where $\delta(x)$ is the delta function. We will use the singular solution of the corresponding steady problem which gives a finite displacement jump when $x \to -\infty$ and infinite stresses at the crack tip $x = 0$.[3] The following notation is used: $\Delta U_x(x, x_0)$ is the displacement jump and $\sum_{zx}(x, x_0)$ are the stresses ahead of the front, determined by this solution. For the derivative $d\Delta U_x(x, x_0)/dx$ behind the front and the stresses ahead of the front we have

$$\frac{d\Delta U_x(x,x_0)}{dx} = \frac{C}{\pi\mu}\left[\sin(\pi\gamma)\left(\frac{x_0}{x}\right)^{\gamma}\frac{1}{x-x_0} + \pi\cos(\pi\gamma)\delta(x-x_0)\right], \quad x \leq 0 \tag{1.1}$$

$$\Sigma_{zx}(x,x_0) = -\frac{1}{\pi}\sin(\pi\gamma)\left(\frac{-x_0}{x}\right)^{\gamma}\frac{1}{x-x_0}, \quad x \geq 0 \tag{1.2}$$

Here,

$$C = C(\upsilon/\beta,\nu) = \begin{cases} 2c_2(1-c_2^2)\left|-4c_1c_2 + (1+c_2^2)^2\right|^{-1}, & \upsilon/\beta < 1 \\ 2c_2(1+c_2^2)[16c_1^2c_2^2 + (1-c_2^2)^4]^{-1/2}, & \upsilon/\beta > 1 \end{cases}$$

$$\gamma = \begin{cases} 1/2, & \upsilon < \upsilon_R \\ -1/2, & \upsilon_R < \upsilon < \beta \\ \dfrac{1}{\pi}\operatorname{arctg}\dfrac{4c_1c_2}{(1-c_2^2)^2}, & \beta < \upsilon < \alpha \end{cases}$$

$$c_1 = \sqrt{1-(\upsilon/\alpha)^2}, \quad c_2 = \sqrt{\left|(\upsilon/\beta)^2 - 1\right|}, \quad \alpha = \sqrt{(2-2\nu)/(1-2\nu)}\,\beta, \quad \beta = \sqrt{\mu/\rho}$$

μ is the shear modulus, ν is Poisson's ratio, α is the velocity of the longitudinal waves, β is the velocity of the transverse waves, ρ is the density and υ_R is the velocity of a Rayleigh wave.

Note that the term generated by the second term in the square brackets on the right-hand side of the equality (1.1) is omitted in formula (6.4) of Ref. 2, corresponding to the singular solution (1.1). It vanishes when $\gamma = ½$. This additional term, which is far from easy to discover, appears in formula (73) of Ref. 1 although, as mentioned above, the main part of the singular solution for a concentrated force was selected using another method.

When $x \to +0$, the singular solution (1.2) has the asymptotic form

$$\Sigma_{zx}(x,x_0) = K_{\mathrm{II}u}(x_0)/(2\pi x)^{\gamma}$$

where $K_{\mathrm{II}u}$ is the stress intensity factor (SIF) corresponding to an isolated concentrated force at the point x_0:

$$K_{\mathrm{II}u}(x_0) = -\frac{2\sin(\pi\gamma)}{[2\pi(-x_0)]^{1-\gamma}} \tag{1.3}$$

When $\gamma = 1/2$, that is, when $v < v_R$, it becomes the conventional stress intensity factor corresponding to the root singularity at the crack tip. In this case, Eq. (1.1) becomes the equation for the static problem if the shear modulus μ is replaced by the value

$$\mu_* = \frac{\mu}{2(1-\nu)C(v/\beta, \nu)}$$

The solution (1.1), (1.2) enables us to consider an arbitrary load distribution behind the crack front: it is sufficient to multiply by the magnitude of the stress and integrate with respect to x_0.

We assume that, at a sufficient distance from the front, the stresses on the sides of the crack are restored to the level of the initial stresses, which are identical to the stresses acting at infinity.

In view of the linearity of the equations of the theory of elasticity, superpositioning can be used. We shall therefore assume that external loads are directly applied to the sides of the crack. The shear stresses σ_e, which arise from these loads, are then non-zero in a certain zone of dimension L which follows the crack tip ($-L < x < 0$). Using definition (1.3), we obtain that the SIF corresponding to external loads is given by the formula

$$K_{IIe} = -2\sin(\pi\gamma)\int_{-L}^{0}\sigma_e(x_0)\frac{dx_0}{[2\pi(-x_0)]^{1-\gamma}} \tag{1.4}$$

Similarly, when calculating the contribution to the SIF from the stresses arising in the end zone as a result of the interaction of the sides of the crack, only the difference σ_i' between the initial and the residual shearing strength can be taken into account. The corresponding SIF is expressed by the formula

$$K_{IIi} = -2\sin(\pi\gamma)\int_{-a}^{0}\sigma_i(x_0)\frac{dx_0}{[2\pi(-x_0)]^{1-\gamma}} \tag{1.5}$$

where a is the size of the end zone.

The actual stresses at the crack tip are limited by the ultimate strength and, in taking account of the interaction of the sides of the crack, the overall SIF must vanish

$$K_{IIe} + K_{IIi} = 0 \tag{1.6}$$

From relations (1.4) - (1.6), we have

$$2\sin(\pi\gamma)\int_{-a}^{0}\sigma_i(x_0)\frac{dx_0}{[2\pi(-x_0)]^{1-\gamma}} = -2\sin(\pi\gamma)\int_{-L}^{0}\sigma_e(x_0)\frac{dx_0}{[2\pi(-x_0)]^{1-\gamma}} \tag{1.7}$$

The condition for of the stresses (1.7) to be finite determines the size of the zone a as a function of the external loads. This is a unique condition which introduces the external loads into the treatment. It follows from this condition that the common factor $2\sin(\pi\gamma)/(2\pi)^{1-\gamma}$, appearing in the definition of the SIF (1.3), does not affect the solution of the problem although it does affect the asymptotic behaviour of the stresses. It is therefore advisable to write the expression for the SIF (1.4) in the form

$$K_{IIe} = -\frac{2\sin(\pi\gamma)}{(2\pi)^{1-\gamma}}K_{II0} \tag{1.8}$$

where

$$K_{II0} = \int_{-L}^{0}\sigma_e(x_0)\frac{dx_0}{(-x_0)^{1-\gamma}} \tag{1.9}$$

We shall call the quantity K_{II0} the *effective* SIF. It is the effective SIF rather then the SIF (1.4) obtained from an analysis of the asymptotic form of the stresses at the crack tip which actually determines the relation between the solution of the problem and the external loads. Its provisional value is given by the product of the characteristic external stress σ_e and L^γ, where L is the characteristic dimension of the domain in which the stresses are restored to the level of the initial stresses:

$$K_{II0} \approx \sigma_e L^\gamma \tag{1.10}$$

We now introduce the dimensionless coordinate $\eta = -x_0/a$. Then, taking of expression (1.8) into account, the condition for the stresses (1.7) to be finite takes the form

$$a^\gamma\int_0^1\sigma_i^*(\eta)\frac{d\eta}{\eta^{1-\gamma}} = K_{II0}; \quad \sigma_i^*(\eta) = \sigma_i(-a\eta) \tag{1.11}$$

Condition (1.11) enables us to investigate the effect of external loads after the equation, obtained by multiplying equality (1.1) by the magnitude of the external σ_e and internal σ_i loads has been solved and integrated with respect to x_0. As a result of integrating the stresses σ_e and σ_i, transformations taking account of condition (1.6), which are similar to the transformations used earlier[10] for the subsonic velocity,

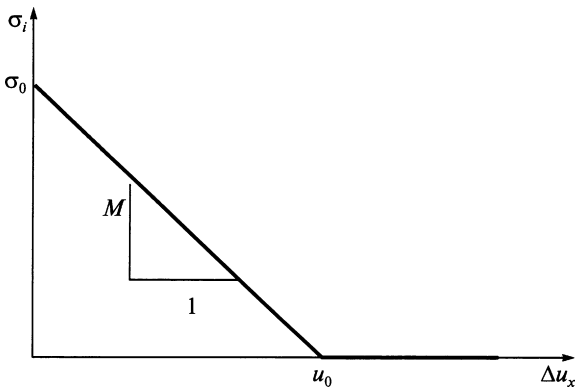

Fig. 2.

and changing to the dimensionless coordinate $\xi = -x/a$, we obtain (see the Appendix) for points in the end zone and close to it behind the crack front

$$\frac{d\Delta u_x^*(\xi)}{d\xi} = \frac{aC}{\pi\mu}\sin(\pi\gamma)\left[\int_0^1 \left(\frac{\xi}{\eta}\right)^{1-\gamma}\frac{\sigma_i^*(\eta)}{\xi-\eta}d\eta - \pi\operatorname{ctg}(\pi\gamma)\sigma_i^*(\xi)\right], \quad \xi \geq 0$$

$$\Delta u_x^*(\xi) = \Delta u_x(-a\xi) \tag{1.12}$$

We now introduce the kernels

$$G_{1-\gamma}(\eta,\xi) = \int_0^{\eta/\xi}\frac{d\varsigma}{\varsigma^{1-\gamma}(1-\varsigma)}$$

$$K(\xi,\eta) = G_{1-\gamma}(\eta,\xi) - \pi\operatorname{ctg}(\pi\gamma)H(\eta/\xi-1), \quad H(\eta/\xi-1) = \begin{cases}0, & \eta<\xi\\ 1, & \eta>\xi\end{cases}$$

where, when $\eta > \xi$, the integral in the definition of $G_{1-\gamma}(\eta, \xi)$ is understood in the sense of a principal value. Then, after integrating equality (1.12) by parts, taking account of the fact that the stress vanishes on the rear boundary of the end zone ($\sigma_i^*(1) = 0$), we obtain

$$\frac{d\Delta u_x^*(\xi)}{d\xi} = -\frac{aC}{\pi\mu}\sin(\pi\gamma)\int_0^1 K(\xi,\eta)\frac{d\sigma_i^*}{d\eta}d\eta, \quad \xi \geq 0 \tag{1.13}$$

We use the law of interaction between the sides of the crack in the end zone. For the linear softening model (Fig. 2), we have

$$\sigma_i = \begin{cases}\sigma_0 - M\Delta u_x, & 0 \leq \Delta u_x \leq u_0\\ 0, & \Delta u_x \geq u_0\end{cases} \tag{1.14}$$

where σ_0 is the shearing strength, M is the softening modulus and u_0 is the maximum displacement at which complete rupture of the bonds occurs ($u_0 = \sigma_0/M$). We now introduce the dimensionless stresses $\sigma = \sigma_i^*/\sigma_0$ and displacement jump $\Delta u = \Delta u_x^*/u_0$. Differentiating equality (1.14) with respect to η and substituting the result into relation (1.13), we obtain the homogeneous equation

$$\frac{d\Delta u(\xi)}{d\xi} - \lambda(\gamma)\int_0^1 K(\xi,\eta)\frac{d\Delta u}{d\eta}d\eta = 0, \quad 0 \leq \xi \leq 1 \tag{1.15}$$

where

$$\lambda(\gamma) = \frac{C}{\pi}\frac{Ma}{\mu}\sin(\pi\gamma) \tag{1.16}$$

The problem has therefore been reduced to finding for the smallest positive number λ_C and the corresponding eigenfunction $g(\xi)$. According to equality (1.6), the dimensionless length $a_n = aM/(2\mu)$ of the end zone is expressed in terms of the eigenvalue by the formula

$$a_n = \frac{aM}{2\mu} = \frac{\varphi(\gamma)}{C}; \quad \varphi(\gamma) = \frac{\pi}{2}\frac{\lambda_C(\gamma)}{\sin(\pi\gamma)} \tag{1.17}$$

($\varphi(\gamma)$ is a function of only the parameter γ).

We find the displacement jump by integrating the eigenfunction $g(\xi)$ and normalizing the result by the value of $g(1)$, which ensures that the discontinuity is equal to the limit value u_0 on the rear boundary of the end zone:

$$\Delta u(\xi) = \frac{\Delta u_x^*}{u_0} = \frac{1}{A}\int_0^\xi g(\xi)d\xi; \quad A = \int_0^1 g(\xi)d\xi$$

The dimensionless stresses in the end zone are determined by the equality

$$\sigma(\xi) = 1 - \Delta u(\xi) \tag{1.18}$$

The relation between the solution and the external load is given by substituting the stresses which have been found into the condition for the stresses to be finite (1.11). In the normalized variables, this condition takes the form

$$\left(\frac{2\mu}{M}\right)^\gamma f_{II} = \frac{K_{II0}}{\sigma_0}; \quad f_{II} = a_n^\gamma \int_0^1 \sigma(\eta)\frac{d\eta}{\eta^{1-\gamma}} \tag{1.19}$$

The quantity f_{II} depends on the normalized velocity υ/β and Poisson's ratio.

2. Analysis of Eq. (1.15). Numerical results and their discussion

Equation (1.15) is a Fredholm equation. In fact, it can be shown that

$$G_{1-\gamma}(\eta,\xi) = \pi\,\mathrm{ctg}(\pi\gamma) + G_\gamma(\xi,\eta)$$

Using this formula and representing the integral along the segment [0,1] as the sum of the integrals along the segments [0,ξ] and [ξ, 1], after some reduction we obtain

$$K(\xi,\eta) = \begin{cases} \frac{1}{\gamma}\left(\frac{\eta}{\xi}\right)^\gamma - \ln\left(1-\frac{\eta}{\xi}\right) - F_\gamma\left(\frac{\eta}{\xi}\right), & \eta \le \xi \\ \frac{1}{1-\gamma}\left(\frac{\xi}{\eta}\right)^{1-\gamma} - \ln\left(1-\frac{\xi}{\eta}\right) - F_{1-\gamma}\left(\frac{\eta}{\xi}\right), & \eta \ge \xi \end{cases}; \quad F_\omega(\zeta) = \int_0^\zeta \frac{1-\zeta^\omega}{1-\zeta}d\zeta, \quad 0 \le \zeta \le 1 \tag{2.1}$$

It follows from this that, when $0 < \gamma \le 1/2$, the kernel of the equation only has a logarithmic singularity at the point $\eta = \xi$ and is therefore of the Fredholm type. Investigation shows that its eigenvalues are positive. The eigenfunctions, corresponding to the eigenvalues, only give physically admissible values of the normalized displacements in the interval [0,1] in the case of the smallest eigenvalue. According to expression (1.17), this smallest eigenvalue determines the normalized size of the end zone.

Analysis also shows that, when $\gamma \to 0$, the principal terms of Eq. (1.15) give the equation

$$\frac{d\Delta u}{d\xi} = -\lambda(\gamma)\pi\mathrm{ctg}(\pi\gamma)(1-\Delta u)$$

Integrating this equation, subject to the condition that $\Delta u(1) = 1$, we obtain

$$\Delta u(\xi) = \exp[-\lambda(\gamma)\pi\mathrm{ctg}(\pi\gamma)(1-\xi)] \tag{2.2}$$

that is, in the case of small γ, the displacement jump changes exponentially close to the rear boundary of the end zone ($\xi = 1$). At the same time, we always have a power asymptotic form of the form $\Delta u(\xi) = O(\xi^{2-\gamma})$ at the crack tip ($\xi = 0$).

When $\gamma = ½$, the function $F_{1/2}(\zeta)$ is expressed by the analytical relation

$$F_{1/2}(\zeta) = 2\left[\sqrt{\zeta} - \ln\left(1+\sqrt{\zeta}\right)\right]$$

In this case, Eq. (1.15) is equivalent to the equations considered earlier.[9–11] In the range between the velocity of a Rayleigh wave and the velocity of transverse waves $\gamma = -1/2$ and, in this case, the kernel has a non-integrable singularity and a solution of the problem does not exist. We therefore arrive at the well known conclusion[1–3] that the propagation of a shear crack with a velocity in the range between the velocity of a Rayleigh wave and the velocity of transverse waves is impossible.

It remains to consider motion with an intersonic velocity. In this case, the function $F_\omega(\zeta)$ and its primitive have to be found numerically. In obtaining the results presented below, the numerical integration was carried out using a fourth-order Runge–Kutta method (for example, see Ref. 12). Double precision arithmetic was used. In the basic calculations, the integration step was 10^{-3} and, as a check, the calculations were also carried out with a step size of 10^{-4} and 10^{-5}. The results of the integrations using the different step sizes were compared with one another and with the analytical expressions corresponding to $\gamma = 0, ½, 1$. As a check, some of the calculations were carried out using an alternative method, an expansion in series. Agreement to no less than six significant figures was always ensured in this case. The eigenvalue and the eigenfunction were subsequently found by iterations of the power method for the algebraic equation obtained after replacing the integral in Eq. (1.15) by a sum using the trapezium formula. Interpolation between the values of the primitive kernel (2.1), calculated by the Runge–Kutta method, was used here. The number of nodes of the quadrature formulae, that is, the number of equations of the homogeneous algebraic system, was varied from 100 to 500. The number of iterations was chosen such that no less than six significant figures were identical for the last five iterations. Finally, as a comparison of the results obtained for a different order of the algebraic system showed, the eigenvalue and eigenvector have no less than four true significant figures.

Table 1

γ	10^{-5}	10^{-4}	10^{-3}	10^{-2}	0.1	0.2	0.3	0.4	0.5
λ_c	$1.40\cdot10^{-4}$	0.00111	0.00878	0.05835	0.2714	0.3737	0.4285	0.4567	0.4655
φ	6.9916	5.5565	4.3892	2.9180	1.3798	0.9987	0.8319	0.8319	0.7311

The values of the eigenvalue $\lambda_C(\gamma)$ and the eigenfunction $\varphi(\gamma)$, determined by the second formula of (1.17) are presented below in Table 1.

It can be seen that the eigenvalue tends to zero when $\gamma \to 0$. However, the limit of the function $\varphi(\gamma)$ is non-zero, which indicates that $\lambda_C(\gamma) = O(\gamma)$. We take account of the fact that the function $C(\upsilon/\beta, \nu)$ in the denominator of the right-hand side of the first equality of (1.17) vanishes on the left boundary of the intersonic range ($\upsilon = \beta$) and is non-zero on its right boundary ($\upsilon = \alpha$). It then follows from the data presented above and formula (1.17) that the dimensionless length a_n of the end zone tends to infinity when the velocity of the crack tends to the velocity of transverse waves and remains finite when the velocity of the crack tends to the velocity of longitudinal waves.

A graph of the dependence of a_n on velocity in the intersonic range is presented in the left upper part of Fig. 3. To be specific, it was constructed for a Poisson's ratio $\nu = 1/4 (\alpha/\beta = \sqrt{3})$. It is clear that in accordance with the above analysis, the size of the end zone increases sharply when $\upsilon \to \beta$. As the velocity of the crack increases, the size of the zone decreases up to a small neighbourhood of the velocity of longitudinal waves at which there is a minimum. When $\upsilon = \sqrt{2}\beta$ which corresponds to $\gamma = ½$, we have $a_n = 0.4223$. The same result was presented earlier in Ref. 9 for this case. When $\upsilon \to \alpha$, the dimensionless length, calculated using the data presented above for the smallest value of $\gamma = 10^{-5}$, is equal to 0.8240.

Graphs of the dimensionless displacements for different values of γ are represented by the solid lines in the lower right part of Fig. 3. Those of them which correspond to values of γ from 0.1 to 0.5 practically coincide with the graphs presented earlier.[1] The graphs for small values of γ are presented for the first time. It is interesting to compare them with the asymptotic form predicted by the analytical relation (2.2) for points close to the rear boundary of the end zone ($\xi = 1$). The corresponding graph for $\gamma = 0.01$ is given by the dashed line. The good agreement between the asymptotic relation and the calculated values close to the rear boundary of the end zone ($\xi = 1$) can be seen: the relative error in the asymptotic formula does not exceed 5% when $\xi > 0.6$. For smaller values of γ, the graphs for the calculated and the asymptotic discontinuities in the displacements are indistinguishable. We emphasize, however, that, close to the crack tip ($\xi < 0.3$), the curves are only indistinguishable because the discontinuities in the displacements tend to zero. As was mentioned, the asymptotic behaviour of the discontinuities in the displacements in this region always follows the relation $\Delta u(\xi) = O(\xi^{2-\gamma})$. The stress distribution in the end zone is given by equality (1.18).

According to equality (1.19), the relation between the solution obtained and the external loads is determined in the first place by the function f_{II}. Its graph, for Poisson's ratio equal to 1/4, is shown in Fig. 4. It follows from the results of the calculations that, over a large part of the intersonic range, the function f_{II} is close to unity and has a weak minimum when $\upsilon/\beta = 1.560$. It increases sharply, tending to infinity, when the velocity of the crack approaches the velocity of transverse or longitudinal waves. This means that the external load, necessary

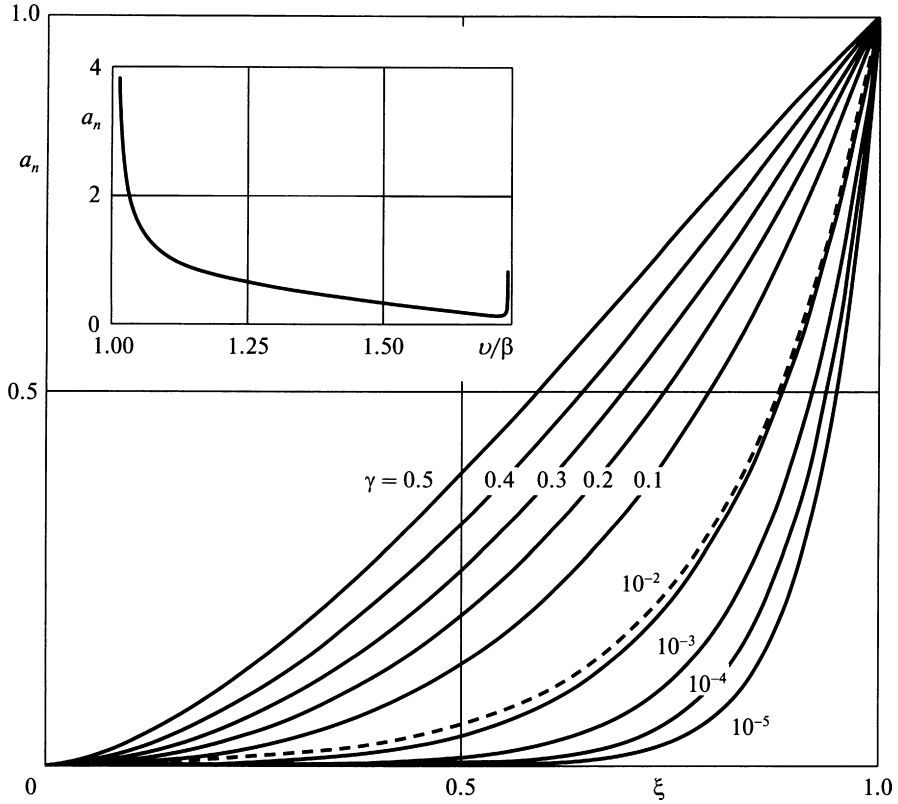

Fig. 3.

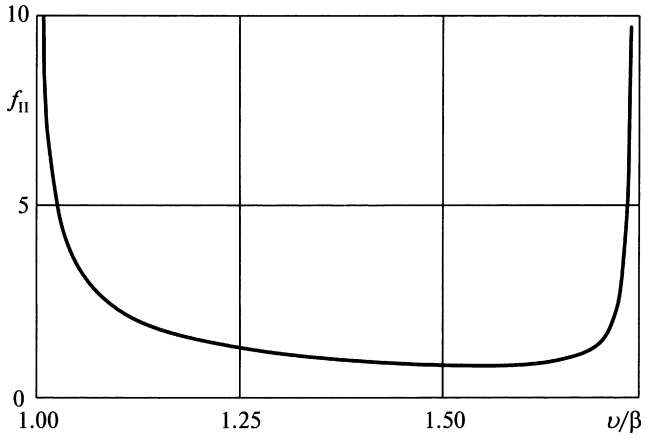

Fig. 4.

for the crack to progress, decreases sharply with an increase in the velocity at the beginning of the intersonic range and increases sharply at the end of this range. Consequently, the neighbourhood of the right-hand end of the intersonic range, that is, motion with a velocity close to the velocity of longitudinal waves, corresponds to stable propagation of a crack.

The actual value of the velocity depends on the properties of the material and the external loads. We will use estimate (1.10) to analyse of this relation. Equality (1.19) then takes the form

$$\frac{\sigma_0}{\sigma_e}\left(\frac{2\mu}{ML}\right)^{\gamma} f_{II} = 1 \tag{2.3}$$

We will now take account of the fact that the crack begins to propagate under a static state when the following condition is satisfied (for example, see Ref. 15)

$$K_{IIS}{}^2(1-\nu)/(2\mu) = \sigma_0^2/(2M)$$

where $K_{IIS} = \sigma_e\sqrt{\pi L_0/2}$ is the static SIF, L_0 is the initial length of the crack and the right-hand side of the condition expresses the energy a per unit area expended on fracturing. At the beginning of the growth, we have

$$\frac{\sigma_0}{\sigma_e}\left(\frac{2\mu}{ML_0}\right)^{1/2} = \sqrt{\pi}$$

where the external stress σ_e is smaller and, as a rule, significantly smaller than the strength of the material σ_0 and, correspondingly, the ratio $2\mu/(ML_0)$ is considerably greater than unity. When account is taken of these considerations, Eq. (2.3) can be written in the form

$$\left(\frac{2\mu}{ML_0}\right)^{\gamma-1/2} f_{II} = \frac{1}{\sqrt{\pi}}\left(\frac{L}{L_0}\right)^{\gamma} \tag{2.4}$$

The parameter γ is close to ½ over a large part of the intersonic range. At the same time the factor on the function f_{II} on the left-hand side of equality (2.3) is close to unity. Then, until the size of the propagating crack exceeds its initial length by more than four times, it follows from equality (2.3) and the graph in Fig. 4 that the velocity of stead motion is located in the middle part of the intersonic range beyond the minimum point $\upsilon/\beta = 1.550$. when its length increases further, crack propagation velocity approaches the velocity of longitudinal waves.

3. Comparison with the Leonov–Panasyuk–Dugdale model

We will now consider the approximation of the softening law in the end zone by the step-function

$$\sigma_i = \begin{cases} \sigma_{0S}, & 0 \le \Delta u_x \le u_{0S} \\ 0, & \Delta u_x \ge u_{0S} \end{cases} \tag{3.1}$$

This approximation corresponds to the Leonov–Panasyuk–Dugdale (LPD) model.[13,14]

For comparison with the results obtained above, we use the values of σ_{0S} and u_{0S}, which give the same energy per unit area for the fracture of the material ($2g = \sigma_0 u_0/2 = = \sigma_{0S}u_{0S}$) and the same ratio of the strength to the limiting displacement ($M = \sigma_0/u_0 = = \sigma_{0S}/u_{0S}$).

Then,

$$\sigma_{0S} = \sigma_0/\sqrt{2}, \quad u_{0S} = u_0/\sqrt{2}$$

The solution of the problem for relation (3.1) is considerably simpler than in the case of the linear softening model (1.14). Substitution of function (3.1) into equality (1.12) and integration leads to an analytical expression for the displacement jump on the rear boundary of

the end zone

$$\Delta u_x(1) = \frac{a_S \sigma_{0S} C}{\pi\mu} \frac{\sin(\pi\gamma)}{1-\gamma} \tag{3.2}$$

The maximum displacement $u_{0S} = \sigma_{0S}/M$ is reached on this boundary, and formula (3.2) therefore gives

$$a_{nS} = \frac{\pi}{2C} \frac{1-\gamma}{\sin(\pi\gamma)} \tag{3.3}$$

for the normalized length of the end zone $a_{nS} = a_S M/(2\mu)$.

Comparison of equalities (3.3) and (1.17) shows that the formulae for the dimensionless length have the same form if

$$\lambda_{CS}(\gamma) = 1 - \gamma$$

is taken as the eigenvalue for the model considered.

For the ratio of the lengths, we have

$$a_n/a_{nS} = \lambda_C(\gamma)/(1-\gamma)$$

Using the numerical data presented in Table 1, we see that, when $\gamma = ½$, the difference between a_{nS} and a_n is 7.5%. Over a large part of the intersonic range where $\gamma = ½$, the LPD model therefore gives approximately the same results as the linear softening model. However, there are differences close to the boundaries of this range where γ tends to zero since, unlike the eigenvalue $\lambda_C(\gamma)$, the function $1-\gamma$ tends to unity rather than to zero. This is not very important close to the left boundary ($v = \beta$), since the function C tends to zero on approaching this boundary and, consequently, a_{nS}, like a_n, tends to infinity although considerably more rapidly. However, the difference is very close to the right boundary ($v = \alpha$) since $C \neq 0$ on this boundary. It follows from this that, unlike in the case of the linear softening model, the length of the end zone in the LPD model increases without limit in the case of a crack velocity approaching he velocity of longitudinal waves.

The dependence of the crack propagation velocity on the external loads is investigated in a similar manner to the case of linear softening. The conclusions drawn from the investigation are also similar. In particular, velocities close to the velocities of longitudinal waves correspond to stable propagation.

Acknowledgement

This research was financed by the Russian Foundation for Basic Research (06-01-00107), 06-05-64089).

Appendix A. Derivation of the basic equation for the end zone

The displacement jump on the surface of a crack is caused by the sum of the external forces $\sigma_e(x)$ and the forces $\sigma_i(x)$ in the end zone. Since the end zone is assumed to be small, the region where the external forces mainly act can be assumed to be separated from the crack tip. To be specific and with the aim of shortening the calculations, we will assume[1] that the external action is due to a concentrated force $\sigma_e(x) = P\delta(x - x_P)$. It acts at a point $x_P = -l$, which follows the crack front at a distance l and, moreover, this distance is considerably greater than the size of the end zone ($l \gg a$). Then, applying the singular solution (1.1) to the external concentrated load $\sigma_e(x)$ and to the distributed load $\sigma_i(x)$ in the end zone, we obtain that their combined action gives the following relation for the derivative of the displacement jump

$$\frac{d\Delta u_x(x)}{dx} = \frac{C}{\pi\mu}\sin(\pi\gamma)\left\{P\left[\left(\frac{x_P}{x}\right)^{\gamma}\frac{1}{x-x_P} + \pi\,\mathrm{ctg}(\pi\gamma)\delta(x-x_P)\right] + \right.$$
$$\left. + \int_{-a}^{0}\sigma_i(x_0)\left[\left(\frac{x_0}{x}\right)^{\gamma}\frac{1}{x-x_0} + \pi\,\mathrm{ctg}(\pi\gamma)\delta(x-x_0)\right]dx_0\right\} \tag{A1}$$

According to formula (1.3), the SIF caused by the concentrated load P is equal to

$$K_{IIe}(x_P) = PK_{IIu}(x_P) = -\frac{2\sin(\pi\gamma)}{[2\pi(-x_P)]^{1-\gamma}}P$$

Using this expression and equality (1.5) in condition (1.6), we have

$$\frac{P}{[2\pi(-x_P)]^{1-\gamma}} = -\int_{-a}^{0}\sigma_i(x_0)\frac{dx_0}{[2\pi(-x_0)]^{1-\gamma}}$$

It follows from this that

$$P\left(\frac{x_P}{x}\right)^{\gamma}\frac{1}{x-x_P} = \frac{x_P}{x-x_P}\frac{1}{(-x)^{\gamma}}\int_{-a}^{0}\sigma_i(x_0)\frac{dx_0}{(-x_0)^{1-\gamma}} \tag{A2}$$

for the first term in the expression in the first square brackets on the right-hand side of equality (A1).

For points of the end zone and close to it $\frac{x}{x_P} \ll 1$, and we replace the ratio $\frac{x_P}{x-x_P}$ in formula (A2) by minus one. Substitution of the resulting approximate expression into formula (A1), integration of the delta function and grouping of the terms after introducing the dimensionless variables

$$\xi = -x/a, \quad \eta = -x_0/a$$

and the functions of them

$$\Delta u_x^*(\xi) = \Delta u_x(-a\xi), \quad \sigma_i^*(\xi) = \sigma_i(-a\xi)$$

leads to the final expression for the derivative of the displacement jump at points of the end zone and close to it, which take the form of equality (1.12).Here, this equality is obtained for the case when the external load is specified to be a concentrated force. However, it can be shown that it holds in the general case of external loads, if their domain of action considerably exceeds the size of the end zone ($L \gg a$). When $\gamma = ½$, this immediately follows from a result obtained earlier (Ref. 11, formula (8)) which was established for arbitrary external loads. It is important that the right-hand side of equality (1.12) only contains forces acting in the end zone.

Formula (1.12) is applicable for any law of interaction between the sides of a crack in the small end zone. Its use, in conjunction with a specific interaction law, leads to a homogeneous, in general, non-linear, equation. Its smallest eigenvalue determines the size of the end zone, and the corresponding eigenfunction gives the distribution of the displacement jump in it. In the special case of a linear interaction, we have the results presented in Table 1.

References

1. Burridge R, Conn G, Freud LB. The stability of a rapid mode II shear crack with finite traction. *J Geophys Res* 1979;**B84**(5):2210–22.
2. Yu HH, Suo Z. Intersonic crack growth on an interface. *Proc Roy Soc London Ser A* 2000;**456**(1993):223–46.
3. Linkov AM. A theory of rupture pulse on softening interface with application to the Chi-Chi earth-quake. *J Geophys Res* 2006;**111**:B09307.1–14.
4. Andrews DJ. Dynamic plane-strain shear rupture with a slip-weakening friction law calculated by a boundary integral method. *Bull Seismol Soc America* 1985;**75**(1):1–21.
5. Dalguer LA, Irikura K, Riera JD, Chiu HC. The importance of the dynamic source effects on strong ground motion during the 1999 Chi-Chi, Taiwan, earthquake: brief interpretation of damage distribution on buildings. *Bull Seism Soc Amer* 2001;**91**(5):1112–27.
6. Liu C, Lambros J, Rosakis AJ. Highly transient elastodynamic crack growth in a biomaterial inter-face: higher order asymptotic analysis and optical experiments. *J Mech Phys Solids* 1993;**41**(12):1887–954.
7. Lambros J, Rosakis AJ. Shear dominated transonic interfacial crack growth in a biomaterial. I. Experimental observations. *J Mech Phys Solids* 1995;**43**(2):169–88.
8. Singh RP, Lambros J, Shukla A, Rosakis AJ. Investigation of the mechanics of intersonic crack propagation along a biomaterial interface using coherent gradient sensing and photoelasticity. *Proc Roy Soc London Ser A* 1997;**453**(1967):2649–67.
9. Lin'kov AM. The size of the end zone and the propagation velocity of a displacement jump. *Prikl Mat Mekh* 2005;**69**(1):144–9.
10. Linkov AM. On two approaches to asymptotic analysis of subsonic rupture propagation. *J Math and Appl* 2006;**28**:93–100.
11. Lin'kov AM, Tleuzhanov MA. Calculation of local zones of irreversible strains close to the crack tip. *Izv Akad Nauk KirgSSR Fiz-Tekhn i Mat Nauki* 1990;**1**:47–51.
12. Samarskii AA. *Introduction to Numerical Methods*. Moscow: Nauka; 1987.
13. Leonov MYa, Panasyuk VV. Development of the finest cracks in a solid body. *Prikl Mekh* 1959;**5**(4):391–401.
14. Dugdale DS. Yielding of steel sheets containing slits. *J Mech Phys Solids* 1960;**8**(2):100–4.
15. Kachanov LM. *Fundamentals of Fracture Mechanics*. Moscow: Nauka; 1974.

Translated by E.L.S.